A Comparative Analysis of GNSS Processing Services for Static Measurements: Evaluating Accuracy and Stability at Different Observation Periods

Mustafin, M.,[1] Nasrullah, M.[1]* and Abboud, M.[3]
[1]Empress Catherine II Saint Petersburg Mining University, Engineering Geodesy Department, Saint Petersburg Russia, E-mail: mustafin_m@mail.ru, mohammad.nasrallah@liu.edu.lb*
[3]Lebanese International University LIU, Surveying Engineering Department, Beirut, Lebanon
E-mail: mohammad.abboud@liu.edu.lb
Corresponding Author

DOI: https://doi.org/10.52939/ijg.v20i9.3553

Abstract
This study examines the accuracy and stability of three prominent Precise Point Positioning (PPP) services: AUSPOS, Trimble RTX, and OPUS, across varying observation periods from 30 to 180 minutes. Static GNSS data was collected at eight different locations over a three-hour timeframe. The analysis focused on comparing the geocentric coordinates (X, Y, Z) obtained from each service, utilizing metrics such as Root Mean Square Error (RMSE) and standard deviations to assess performance. The results revealed that processing time significantly influences accuracy, with Trimble RTX demonstrating the highest precision across all intervals. AUSPOS displayed considerable variations at shorter observation periods, while OPUS exhibited larger discrepancies, indicating potential challenges in stability. These findings underscore the strengths and weaknesses of each service, offering critical insights for selecting the most appropriate GNSS processing option tailored to specific geodetic applications. By highlighting the relationship between observation duration and positioning accuracy, this study contributes valuable knowledge to the field of geodesy and PPP service utilization.

Keywords: AUSPOS, OPUS, Precise Point Positioning, Static GNSS, Trimble RTX

1. Introduction

Technological advancements in various domains such as geodesy, geotechnical engineering, natural hazard assessment, and ionospheric research have created a growing demand for high-accuracy measurements [1] and [2]. The need for accurate and precise data has become increasingly crucial in applications such as landslide monitoring, underground mining operations, and ionospheric studies, where even small measurement errors can have significant consequences for safety, productivity, and scientific understanding [3][4] and [5]. The Global Navigation Satellite System (GNSS) has transformed the world of positioning and navigation, enabling accurate and reliable location information for a broad range of applications [6][7] and [8]. A constellation of satellites orbiting the Earth transmit radio signals that are received by ground-based receivers, which then calculate the receiver's position, velocity, and time [9][10] and [11]. This technology has become an indispensable tool in modern geodesy, providing precise positioning data for tasks such as surveying, mapping, and monitoring [12][13] and [14]. The accuracy of GNSS solutions depends on several factors, including the quality of the observed data, processing software, and processing time [15][16] and [17]. Various GNSS processing services are available, offering different levels of accuracy and turnaround times [18]. While satellite geometry, signal quality, and atmospheric conditions can affect GNSS positioning accuracy, this technology remains a vital component of modern navigation and spatial awareness [19][20] and [21].

Precise Point Positioning (PPP) services have become a cornerstone of modern geolocation technology, providing high-accuracy positioning information for a wide range of applications. The accuracy of PPP services is unparalleled, with centimeter-level precision, making them an essential tool for industries such as surveying, mapping, and geospatial analysis [22][23] and [24].

One of the key advantages of PPP services is their ability to provide accurate positioning in real-time, allowing for rapid response and decision-making. Additionally, PPP services offer significant cost savings compared to traditional surveying methods, as they eliminate the need for on-site data collection and reduce the requirement for extensive infrastructure setup [25][26] and [27]. Furthermore, PPP services are often simpler to implement and use than other positioning technologies, as they can be easily accessed through online platforms or software applications. For instance, many online mapping platforms and geographic information systems (GIS) now integrate PPP data to provide users with accurate and up-to-date information on their surroundings. With its unparalleled accuracy, simplicity, and cost-effectiveness, PPP has revolutionized the way we understand and interact with our environment [28] [29] and [30].

In the PPP services, a receiver collects GNSS signals from multiple satellites and transmits the data to a central server, which then uses sophisticated algorithms to calculate the receiver's precise position and attitude. PPP services typically utilize a combination of global and local reference stations, as well as advanced models of atmospheric delays and satellite orbits, to achieve accuracy levels of a few centimeters [31][32] and [33]. This study provides an in-depth analysis of three leading Precise Point Positioning (PPP) services, specifically AUSPOS, Trimble RTX, and OPUS, which are renowned for their exceptional accuracy and reliability in providing high-precision geolocation data. So, let's briefly introduce each service to provide a comprehensive understanding of their strengths and capabilities.

Geoscience Australia offers a free online GPS data processing service called AUSPOS, which harnesses the International GNSS Service's global network of stations and products. AUSPOS is capable of processing GPS data collected anywhere on the planet. Users can submit high-quality, dual-frequency GPS data collected in static mode to AUSPOS, which will generate an email report providing coordinates in three different reference frames: Geocentric Datum of Australia 2020 (GDA2020), Geocentric Datum of Australia 1994 (GDA94), and International Terrestrial Reference Frame (ITRF). Trimble RTX is a global navigation satellite system (GNSS) technology that provides extremely accurate positioning, down to centimeters, anywhere in the world at any time. By uploading GNSS observation data to the CenterPoint RTX post-processing service, users can receive precise positioning calculations. These calculations are based on the current reference frame (ITRF2014 for data collected after March 23rd, 2017).

NOAA's Online Positioning User Service (OPUS) offers free access to high-accuracy National Spatial Reference System (NSRS) coordinates. OPUS utilizes the same software used to compute coordinates for the nations geodetic control marks and the NOAA CORS Network (NCN). Despite their widespread use, the performance characteristics of these services for varying observation durations have received limited study. This study aims to address this gap by investigating the accuracy and convergence time of AUSPOS, Trimble RTX, and OPUS for static GNSS measurements of different durations. It's worth noting that all three services, AUSPOS, Trimble RTX, and OPUS, have specific requirements for the uploaded data. Specifically, they all decimate the data to 30-second intervals. The services accept data in a standardized format, specifically Rinex 3 (RINEX). RINEX stands for Receiver Independent Exchange Format, and it is a widely used format for exchanging GNSS observation data between receivers and processing software. Rinex 3 is the third version of this format, which provides a more efficient and flexible way to store and exchange GNSS data.

2. Background Research

Previous studies have shown that the accuracy of PPP is affected by the observation period where longer observation periods typically result in higher accuracy due to the increased number of available satellite observations and reduced effects of noise and multipath interference [34] and [35]. In a previous study in the reference 34, investigation assessed the performance of three global online and free Precise Point Positioning (PPP) services, namely CSRS, APPS, and GMV, using GNSS data collected from four permanent stations located in various regions of Kyrgyzstan. The study analyzed the PPP results and found that the maximum deviations in the planar surface were 2.5 cm and 4.5 cm for 24-hour and 4-hour GNSS observations, respectively. Additionally, under optimal satellite observation conditions, the geodetic height deviations were approximately 10 cm.

Also, the study in the reference 35 tested a horizontal coordinate’s correction model based on the International Terrestrial Reference Frame 2014 (ITRF2014) in Thailand, utilizing the Precise Point Positioning (PPP) technique implemented in GipsyX software. The study employed data from Continuously Operating Reference Stations (CORS) scattered across the country, with coordinates from selected points observed twice and divided into training and check points.

The PPP technique was applied to obtain 3D coordinates for all points, and the training points were used to estimate shift rates between epochs. Previous studies have explored the accuracy and performance of different GNSS processing services, but often focused on specific applications or analyzed data from specific regions. Some studies have investigated the impact of processing time on GNSS accuracy, but not in a comprehensive comparison of popular services like AUSPOS, Trimble RTX, and OPUS. Another study in the reference 36 examined the impact of elevation mask on multi-GNSS kinematic PPP performance. The study concluded that while higher masks generally improve accuracy and speed, a mask below 25 degrees still allows for good accuracy (5 cm horizontal, 10 cm vertical) after 15 minutes of measurements.

In addition, a comprehensive study in the reference 37 investigated the various error sources influencing PPP accuracy, including atmospheric delays, satellite errors, and site displacements. The study emphasized the benefits of dual-frequency PPP for achieving centimeter-level accuracy, supported by both static IGS data and kinematic road test results. While previous research has explored the impact of observation periods and investigated the error sources, a comprehensive analysis comparing popular PPP services across different observation durations is still lacking. Studies often focus on specific applications or regions, leaving a gap in our understanding of the general trends and service-specific behaviors. For example, the impact of processing time on PPP accuracy has been investigated in some studies, but not in a comprehensive comparison of services like AUSPOS, Trimble RTX, and OPUS.

Furthermore, existing research often lacks a detailed investigation into the stability and variability of coordinates over varying observation periods. This information is crucial for understanding the reliability and consistency of PPP solutions over time. To address these research gaps, this study investigates the effect of varying observation periods on the accuracy of PPP in Lebanon using three different PPP services. Unlike previous studies that collected new data, this research utilizes existing raw data from 8 points in Lebanon, divided into intervals ranging from 30 minutes to 180 minutes. By analyzing the coordinate stability and variability across these observation durations, this study contributes to a deeper understanding of the optimal observation period for PPP and its implications for positioning accuracy. The findings have broader implications for PPP implementation strategies and optimization techniques in various GNSS applications worldwide.

3. **Methodology and Results**

3.1 Data Acquisition

We conducted a comprehensive three-hour continuous static GNSS measurement campaign utilizing four TOPCON Hiper V receivers at eight distinct locations. These receivers are equipped to track a full range of satellite constellations, including GPS (L1, L2, and L2C), GLONASS (L1 and L2), and SBAS. After collecting the data from the receivers, we transferred it to a computer and processed it using TOPCON Magnet Tools software. The initial stage of this process involved defining the antenna type, specifying the antenna height, and assigning a name to each measurement point. In the subsequent stage, we converted the collected data into the RINEX 3 format and exported it as a new file. The final stage involved splitting the three-hour RINEX file into six segments of varying durations—30, 60, 90, 120, 150, and 180 minutes. We accomplished this by utilizing the "Split" tool, which allowed us to input the desired segment duration in minutes. This splitting process was replicated multiple times for each measurement point to ensure we could accommodate the required observation periods. The resulting RINEX 3 files were then exported and prepared for upload to Precise Point Positioning (PPP) services. The Figure 1 shows the distribution of the observed points in the territories of the Lebanese Republic.

3.2 Data Processing

After completing the data segmentation process, we uploaded each segment to AUSPOS and Trimble RTX to obtain precise positioning solutions. To access the AUSPOS service, users can navigate to the website at https://gnss.ga.gov.au/auspos. Once there, they should upload the RINEX file, and upon clicking the "Scan" button, the system will automatically recognize the antenna type and height. Users are then required to enter their email address and click "Submit." They will receive two emails: the first confirming that the analysis has begun, accompanied by a specific job number, and the second containing a PDF report with the submitted results. The Trimble RTX service can be accessed via https://trimblertx.com/UploadForm.aspx. Here, users must select the coordinate system, specify the tectonic plate, upload the appropriate file, enter their email address, and finally click the "Process" button. The server will then send an email with a PDF report that includes the submission results. In our study, we specifically selected the ITRF 2014 coordinate system and the "Arabia" tectonic plate, as the measurements were conducted in Lebanese territory.

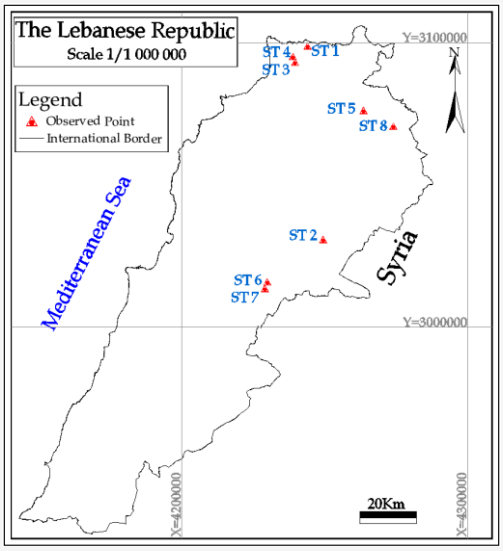

Figure 1: Distribution of observed points in the Lebanese Republic

Additionally, we uploaded segments of 120 minutes, 150 minutes, and 180 minutes to OPUS, which requires a minimum observation period of two hours for processing. The emails received from this service indicated an "aborted" status for the shorter observation periods. Users can access OPUS at https://www.ngs.noaa.gov/OPUS/. On this platform, they must choose the file to upload, select the antenna type from the provided list, input the antenna height and email address, and click the “Upload to Static” button. Following processing, OPUS sends an email containing the results of the submission. After completing the processes with AUSPOS, Trimble RTX, and OPUS, we downloaded the resulting solutions and extracted the geocentric coordinates (X, Y, Z) for further analysis.

4. Data Analysis

Based on the obtained geocentric coordinates from the 3 services at the selected observation time intervals, the analysis are done taking into account multiple considerations. The graph in Figure 2 presents the average differences in geocentric coordinates between AUSPOS, Trimble RTX, and OPUS for the eight points observed at the 180-minute mark. This chart provides a visual representation of the average differences in X, Y, and Z coordinates between the three services at this specific observation interval. Table 1 presents the coordinates absolute deviations from 180-minute marks for AUSPOS at eight points. These values represent the absolute differences between the actual coordinate values at each point and their corresponding values at the 180-minute mark. The table provides a detailed breakdown of these deviations, allowing for a closer examination of the discrepancies. At the end of this table, we also include the mean absolute deviations for each coordinate (X, Y, and Z) across all eight points.

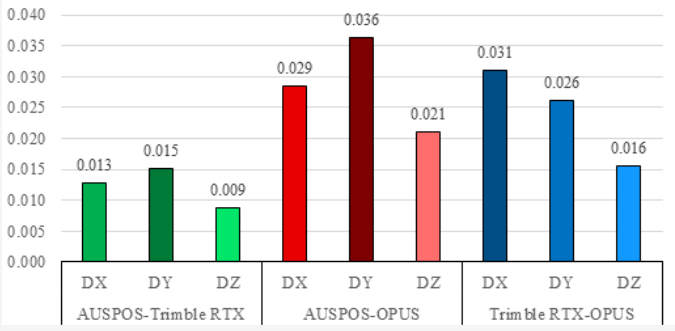

Figure 2: Comparison of the results of the used PPP platforms at 180-minute observation interval

Table 1: Coordinates absolute deviations from 180-minute marks for AUSPOS results

Point	Coordinates Absolute Deviations from 180 minutes Marks at specified observations interval					
	Coordinate	**30 m**	**60m**	**90m**	**120m**	**150m**
ST1	X	0.099	0.075	0.004	0.002	0.007
	Y	0.018	0.014	0.005	0.000	0.001
	Z	0.001	0.019	0.007	0.003	0.002
ST2	X	0.028	0.009	0.011	0.012	0.009
	Y	0.029	0.002	0.021	0.002	0.001
	Z	0.067	0.004	0.007	0.003	0.001
ST3	X	0.484	0.066	0.013	0.003	0.003
	Y	0.318	0.040	0.011	0.003	0.003
	Z	0.072	0.015	0.002	0.004	0.003
ST4	X	0.092	0.113	0.041	0.001	0.017
	Y	0.166	0.196	0.019	0.002	0.008
	Z	0.028	0.075	0.026	0.003	0.010
ST5	X	0.739	0.060	0.005	0.006	0.004
	Y	1.313	0.028	0.001	0.001	0.000
	Z	0.120	0.041	0.003	0.008	0.001
ST6	X	0.233	0.005	0.014	0.023	0.011
	Y	0.030	0.051	0.057	0.047	0.022
	Z	0.115	0.016	0.007	0.019	0.006
ST7	X	0.203	0.007	0.000	0.005	0.004
	Y	0.037	0.017	0.007	0.006	0.001
	Z	0.097	0.018	0.007	0.001	0.003
ST8	X	0.549	0.168	0.167	0.000	0.001
	Y	0.033	0.170	0.030	0.015	0.009
	Z	0.042	0.053	0.060	0.018	0.004
Mean	X	0.303	0.063	0.032	0.007	0.007
	Y	0.243	0.065	0.019	0.009	0.006
	Z	0.068	0.030	0.015	0.007	0.004

Table 2: Coordinates absolute deviations from 180-minute marks for Trimble RTX results

Point	Coordinates Absolute Deviations from 180 minutes Marks at specified observations interval					
	Coordinate	**30 m**	**60m**	**90m**	**120m**	**150m**
ST1	X	0.023	0.016	0.010	0.004	0.000
	Y	0.027	0.016	0.003	0.005	0.000
	Z	0.006	0.001	0.005	0.003	0.000
ST2	X	0.018	0.020	0.008	0.003	0.001
	Y	0.023	0.021	0.006	0.007	0.004
	Z	0.006	0.009	0.001	0.004	0.003
ST3	X	0.005	0.039	0.003	0.005	0.002
	Y	0.036	0.016	0.014	0.005	0.000
	Z	0.028	0.001	0.006	0.004	0.002
ST4	X	0.010	0.006	0.015	0.012	0.004
	Y	0.035	0.020	0.008	0.011	0.009
	Z	0.013	0.002	0.005	0.008	0.004
ST5	X	0.033	0.066	0.013	0.012	0.009
	Y	0.042	0.013	0.007	0.004	0.004
	Z	0.027	0.066	0.014	0.009	0.001
ST6	X	0.034	0.056	0.020	0.007	0.001
	Y	0.033	0.005	0.022	0.023	0.003
	Z	0.075	0.044	0.008	0.005	0.004
ST7	X	0.014	0.001	0.002	0.007	0.000
	Y	0.005	0.027	0.001	0.001	0.002
	Z	0.022	0.013	0.003	0.002	0.001
ST8	X	0.026	0.035	0.009	0.006	0.011
	Y	0.212	0.072	0.025	0.014	0.011
	Z	0.063	0.000	0.020	0.006	0.011
Mean	X	0.020	0.030	0.010	0.007	0.003
	Y	0.052	0.024	0.011	0.009	0.004
	Z	0.030	0.017	0.008	0.005	0.003

Table 3: Coordinates absolute deviations from 180-minute marks for OPUS results

Point	Coordinates Absolute Deviations from 180 minutes Marks at specified observations interval		
	Coordinate	120m	150m
ST1	X	0.001	0.004
	Y	0.011	0.011
	Z	0.000	0.008
ST2	X	0.044	0.002
	Y	0.039	0.002
	Z	0.030	0.003
ST3	X	0.023	0.007
	Y	0.017	0.004
	Z	0.021	0.006
ST4	X	0.029	0.008
	Y	0.022	0.004
	Z	0.009	0.002
ST5	X	0.026	0.053
	Y	0.051	0.034
	Z	0.018	0.009
ST6	X	0.008	0.034
	Y	0.059	0.089
	Z	0.024	0.039
ST7	X	0.006	0.002
	Y	0.002	0.003
	Z	0.026	0.003
ST8	X	0.086	0.033
	Y	0.009	0.025
	Z	0.050	0.016
Mean	X	0.028	0.018
	Y	0.026	0.021
	Z	0.022	0.011

Table 4: The calculated values of RMSE for the results of the 3 platforms

Platform	RMSE (m)	30 min	60 min	90 min	120 min	150 min
AUSPOS	X	0.387	0.083	0.061	0.010	0.009
	Y	0.482	0.095	0.025	0.018	0.009
	Z	0.078	0.038	0.024	0.010	0.005
Trimble	X	0.023	0.037	0.011	0.008	0.005
	Y	0.080	0.031	0.014	0.011	0.006
	Z	0.038	0.029	0.010	0.006	0.005
OPUS	X	-	-	-	0.038	0.025
	Y	-	-	-	0.033	0.035
	Z	-	-	-	0.026	0.016

Table 5: The calculated values of Standard Deviation for the results of the 3 platforms

Platform	Standard Deviation (m)	30 min	60 min	90 min	120 min	150 min
AUSPOS	X	0.256	0.057	0.056	0.008	0.005
	Y	0.445	0.075	0.018	0.016	0.007
	Z	0.042	0.024	0.020	0.007	0.003
Trimble	X	0.011	0.023	0.006	0.003	0.004
	Y	0.066	0.021	0.009	0.007	0.004
	Z	0.026	0.025	0.006	0.002	0.003
OPUS	X	-	-	-	0.027	0.019
	Y	-	-	-	0.021	0.030
	Z	-	-	-	0.015	0.012

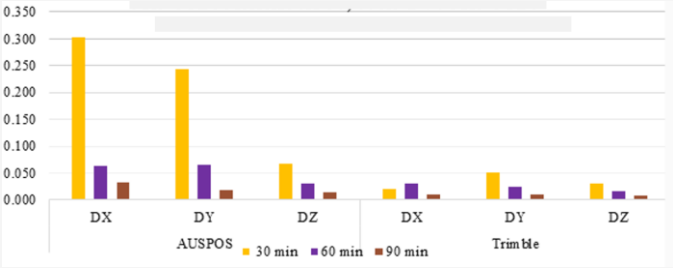

Figure 3: Comparison of the deviations at 30, 60 and 90-minute interval for AUSPOS and Trimble results

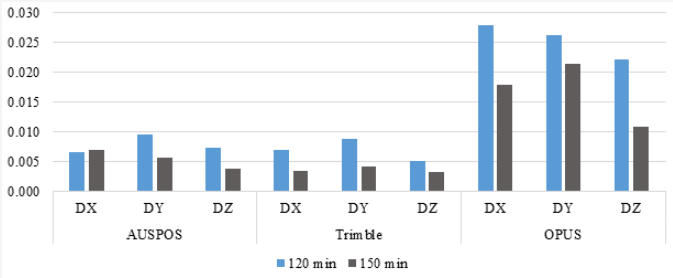

Figure 4: Comparison of the deviations at 120 and 150-minute interval for the results of the 3 platforms

Following the presentation of AUSPOS deviations, we now examine the corresponding deviations for Trimble RTX at the same eight points. The coordinate's absolute deviations from 180-minute marks for Trimble RTX are available in Table 2 of the Appendix, highlighting the differences in accuracy between this service and AUSPOS. Note that we have also calculated the mean absolute deviations for each coordinate (X, Y, and Z) across all eight points, which are presented at the end of this table. Finally, we examine the deviations for OPUS, which only reports at 120m and 150-minute marks. The Table 3 in the Appendix presents the coordinates absolute deviations from these reported marks at the eight points, highlighting the differences in accuracy between OPUS and the other two services. Note that we have also calculated the mean absolute deviations for each coordinate (X, Y, and Z) across all eight points, which are presented at the end of this table. This graph shown in Figure 3 compares the differences in X, Y, and Z coordinates between AUSPOS and Trimble services at intervals of 30, 60, and 90 minutes, with the 180-minute interval serving as a reference. The graph highlights the performance of each service in capturing the variations in GNSS signal reception over time. The graph in Figure 4 showcases the differences in X, Y, and Z coordinates between all three services (AUSPOS, Trimble RTX, and OPUS) at intervals of 120 and 150 minutes with the reference 180 minutes results. The graph provides a comprehensive view of the performance of each service in capturing GNSS signals over relatively longer periods. The Table 4 of the Appendix presents the calculated Root Mean Square Error (RMSE) values for the used PPP services at all intervals based on the results of the 180 minutes intervals, except the non-obtained results of the 30, 60 and 90 minutes intervals of OPUS service. In addition, the Table 5 of the Appendix shows the calculated Standard Deviations also by assuming that the results of the 180 minutes intervals are the target values.

5. Conclusion

The comparison of the mean geocentric coordinates of the GNSS data uploaded to three PPP services reveals an intriguing pattern. While the differences in Z values are generally smaller compared to those in X and Y coordinates, indicating a higher degree of agreement among the three services in terms of vertical position, the analysis shows that AUSPOS and Trimble RTX services exhibit relatively small differences in their coordinate values when compared to each other. In contrast, OPUS service stands out, with significantly larger differences in X, Y, and Z coordinates when compared to the AUSPOS and Trimble services. This suggests that this service may have a unique characteristic or processing approach that affects its positioning accuracy, leading to larger deviations from the other two services.

Also, the comparison of geocentric coordinates from AUSPOS and Trimble PPP services at the 30, 60 and 90-minute intervals with the 180-minute interval reveals distinct patterns. Trimble RTX service exhibits relatively consistent and stable

performance across all intervals, with minimal variations in its coordinate values. In contrast, the AUSPOS service displays noticeable anomalies and variations in its coordinates, particularly at shorter observation time periods (30-60 minutes). These findings suggest that the Trimble service may be more robust to short-term fluctuations in the GNSS signal, while the AUSPOS service may be more sensitive to these variations. Further investigation is needed to understand the underlying causes of these differences in stability and variability.

The comparison of geocentric coordinates from three PPP services at different intervals (120 and 150 minutes) with the 180-minute interval reveals that AUSPOS and Trimble RTX services exhibit small anomalies and good stability, with differences of less than 1 cm between their coordinate values and the 180-minute interval. In contrast, the OPUS service shows larger anomalies, with differences ranging from 1 to 3 cm between its coordinate values and the 180-minute interval. This suggests that the latter service may be more prone to errors or inconsistencies in its positioning solution at shorter observation time periods, while AUSPOS and Trimble RTX demonstrate better stability and accuracy. Finally, the values shown in the calculated RMSE and Standard Deviations show that Trimble RTX exhibits the highest accuracy and precision, AUSPOS results at intervals less than 2 hours show significant anomalies while results of 120 and 150 minutes are more stable, while OPUS requires further studies to clarify the reasons of the relatively high anomalies and inconsistent stability. The results highlight the importance of considering not only the magnitude of errors but also their distribution and relationships between different services when evaluating the performance of GNSS-based positioning solutions.

References

[1] Kitpracha, C., Promchot, D., Srestasathiern, P. and Satirapod, C., (2017). Precise Tropospheric Delay Map of Thailand using GNSS Precise Point Positioning Technique. *International Journal of Geoinformatics*, Vol. 13(2). https://journals.sfu.ca/ijg/index.php/journal/article/view/1031.

[2] Thammaboribal, P., Tripathi, N.K., Ninsawat, S., and Pal, I. (2022). Earthquake precursory detection using diurnal GPS-TEC and kriging interpolation maps: 12 May 2008, Mw7.9 Wenchuan case study, *MethodsX*, Vol. 9; 101617. https://doi.org/10.1016/j.mex.2022.101617.

[3] Marinin, M. A., Rakhmanov, R. A., Alenichev, I. A., Afanasyev, P. I. and Sushkova, V. I., (2023). Effect of Grain Size Distribution of Blasted Rock on WK-35 Shovel Performance. *MIAB. Mining Informational and Analytical Bulletin*, Vol. 6, 111–125. https://doi.org/10.25018/0236_1493_2023_111_0_305.

[4] Kuzin, A. A. and Filippov, V. G., (2023). Development of an Algorithm for Choosing a Method and Geodetic Equipment Depending on the Velocity of Landslide Displacements, by the Example of the Miatlinskaya HPS. *Vestnik SSUGT (Siberian State University of Geosystems and Technologies)*, Vol. 28(4), 22–37. https://doi.org/10.33764/2411-1759-2023-28-4-22-37.

[5] Kornilov, Y. N., Romanchikov, A. Y. and Bogolyubova, A. A., (2023). Estimating Deformation Process through Single Shot Close Range Photogrammetry Method in Agisoft Metashape. *Geodesy and Cartography = Geodezia i Kartografia*, Vol. 84(10), 2-11. https://doi.org/10.22389/0016-7126-2023-1000-10-2-11.

[6] Bui Nhi, T., Tran Van, P., Nguyen Van, D. and Phan Trong, T., (2024). The Present Strain Rate of Quang Nam - Quang Ngai and the Surrounding Region. *Vietnam Journal of Earth Sciences*, Vol. 46(3), 303–321. https://doi.org/10.15625/2615-9783/20400

[7] Charoenphon, C., (2019). Monitoring Precipitable Water Vapor in Real-Time using Kinematic GPS Precise Point Positioning in Thailand. *International Journal of Geoinformatics*, Vol. 15(1). https://journals.sfu.ca/ijg/index.php/journal/article/view/1244.

[8] Mustafin, M., Nasrullah, M. and Abboud, M., (2024). 3D Modeling of Sidon Sea Castle Utilizing Terrestrial Laser Scanner Combined with Photogrammetry. *International Journal of Geoinformatics*, Vol. 20(5), 28–39. https://doi.org/10.52939/ijg.v20i5.3227

[8] Htay, H., Lwin, Z. and Hla, T., (2023). Implementation of Signal Acquisition and Tracking for GPS-Based Software Defined Radio Receiver. *International Journal of Geoinformatics*, Vol. 19(2), 55–64. https://doi.org/10.52939/ijg.v19i2.2567.

[9] Kandil, I., Awad, A. and El-Mewafi, M., (2023). Role of Multi-Constellation GNSS in the Mitigation of the Observation Errors and the Enhancement of the Positioning Accuracy. *International Journal of Geoinformatics*, Vol. 19(4), 25–35. https://doi.org/10.52939/ijg.v19i4.2631.

[10] Mao, X., Wang, W. and Gao, Y., (2024). Precise Orbit Determination for Low Earth Orbit Satellites Using GNSS: Observations, Models, and Methods. *Astrodynamics*, 1-26. https://doi.org/10.1007/s42064-023-0195-z.

[11] Aziz, M., Pa'suya, M., Talib, N., Din, A., Hashim, S. and Ramli, M., (2023). Vertical Accuracy Assessment of Improvised Global Digital Elevation Models (MERIT, NASADEM, EarthEnv) Using GNSS and Airborne IFSAR DEM. *International Journal of Geoinformatics*, Vol. 19(12), 65–82. https://doi.org/10.52939/ijg.v19i12.2979

[12] Almagbile, A., Al-Rawabdeh, A. and Hazaymeh, K., (2023). Analysis of Single and Double Faults Direction and Magnitude in Measurement and State Models of Tight GPS/INS System. *International Journal of Geoinformatics*, Vol. 19(7), 47–62. https://doi.org/10.52939/ijg.v19i7.2745.

[13] Kazantsev, A., Boikov, A. and Valkov, V., (2020). Monitoring the Deformation of the Earth's Surface in the Zone of Influence Construction. *In E3S Web of Conferences*, Vol. 157. https://doi.org/10.1051/e3sconf/202015702013.

[14] Pırtı, A. and Yücel, M., (2023). Evolution of the Accuracy and Performance of Multi-GNSS (MGEX) Positioning for Long Baselines by Using Different Software. *Journal of Geodesy and Geoinformation Science*, Vol. 6(4). https://doi.org/10.11947/j.JGGS.2023.0407.

[15] Kadirov, F., Yetirmishli, G., Safarov, R., Mammadov, S., Kazimov, I., Floyd, M., Reilinger, R. and King, R., (2024). Results of 25 Years (1998-2022) Crustal Deformation Monitoring in Azerbaijan and Adjacent Territory Using GPS. *ANAS Transactions, Earth Sciences*, Vol. 1/2024, 28-43, https://doi.org/10.33677/ggianas20240100107.

[16] Xu, W. A. N. G. and Hongzhou, C. H. A. I., (2023). Developing an Innovative High-precision Approach to Predict Medium-term and Long-term Satellite Clock Bias. *Journal of Geodesy and Geoinformation Science*, Vol. 6(1), 47-58. https://doi.org/10.11947/j.JGGS.2023.0104.

[17] Jiang, W., Qile, Z. H. A. O., Min, L. I., Jing, G. U. O., Jianghui, G. E. N. G., Zhao, L. I., Gu, S. F., Zhang, Q., Hu, Z. and Na, W. E. I., (2023). The Progress of IGS Analysis Center at Wuhan University. *Journal of Geodesy & Geoinformation Science*, Vol. 6(3). https://doi.org/10.11947/j.JGGS.2023.0305.

[18] Li, B., Miao, W. and Chen, G. E., (2023). Key Technologies and Challenges of Multi-frequency and Multi-GNSS High-precision Positioning. *Geomatics and Information Science of Wuhan University*, Vol. 48(11), 1769-1783. https://doi.org/10.13203/j.whugis20230309.

[19] Xu, P., Zhang, G., Yang, B. and Hsu, L. T., (2024). Machine Learning in GNSS Multipath/NLOS Mitigation: Review and Benchmark. *IEEE Aerospace and Electronic Systems Magazine*,1-17, https://doi.org/10.1109/MAES.2024.3395182.

[20] de Paula, E. R.., Monico, J. F. G., Tsuchiya, Í. H., Valladares, C. E., Costa, S. M. A., Marini-Pereira, L., Vani B. C. and Moraes, A. D. O., (2023). A Retrospective of Global Navigation Satellite System Ionospheric Irregularities Monitoring Networks in Brazil. *Journal of Aerospace Technology and Management*, Vol. 15. https://doi.org/10.1590/jatm.v15.1288.

[21] Li, X., Barriot, J. P., Lou, Y., Zhang, W., Li, P. and Shi, C., (2023). Towards Millimeter-Level Accuracy in GNSS-based Space Geodesy: A Review of Error Budget for GNSS Precise Point Positioning. *Surveys in Geophysics*, Vol. 44(6), 1691-1780. https://doi.org/10.1007/s10712-023-09785-w.

[22] Uaratanawong, V., Tangvijitjankarn, K. and Satirapod, C., (2024). Performance of a Low-Cost GNSS Receiver Using MADOCA Corrections with Precise Point Positioning (PPP) Mode in Thailand. *International Journal of Geoinformatics*, Vol. 20(5), 69–78. https://doi.org/10.52939/ijg.v20i5.3233

[23] Farhan, M. and Gomaa, M., (2021). The Improvement in the Positioning on the Nubian and Somalia Plates by Updating Terrestrial Reference Frames. *International Journal of Geoinformatics*, Vol. 17(3), 14–22. https://doi.org/10.52939/ijg.v17i3.1891.

[24] Vystrchil, M. G., Baltyzhakova, T. I., Romanchikov, A. Yu. And Bogolyubova, A. A., (2024). Algorithm of Land Surface Points Extraction from Airborne Laser Scanning Data. *Geodesy and Cartography = Geodezia i Kartografia*, Vol. 85(2), 2-11. https://doi.org/10.22389/0016-7126-2024-1004-2-2-11.

[25] Valkov, V. A., Vinogradov, K. P., Valkova, E. O. and Mustafin, M. G., (2022) Creating highly Informative Rasters Based on Laser Scanning and Aerial Photography Data. *Geodesy and cartography = Geodezia i Kartografia*, Vol. 83(11), 40-49. https://doi.org/ 10.22389/0016-7126-2022-989-11-40-49.

[26] Yuanxi, Y. A. N. G., Xia, R. E. N. and Jianrong, W. A. N. G., (2024). Development of Integrated and Intelligent Geodetic and Photogrammetry Satellites with Corresponding Key Technologies. *Journal of Geodesy and Geoinformation Science*, Vol. 6(4), 3-12. https://doi.org/10.11947/j.JGGS.2023.0401.

[27] Hou, P., Zha, J., Liu, T. and Zhang, B., (2023). Recent Advances and Perspectives in GNSS PPP-RTK. *Measurement Science and Technology*, Vol. 34(5). https://doi.org/10.1088/1361-6501/acb78c.

[28] Stopar, B., Sterle, O., Pavlovčič-Prešeren, P. and Hamza, V., (2024). Observations and Positioning Quality of Low-Cost GNSS Receivers: A review. *GPS Solutions*, Vol. 28(3). https://doi.org/10.1007/s10291-024-01686-8.

[29] Valkov, V. A., Kuzin, A. A. and Kazantsev, A. I., (2018). Calibration of Digital Non-Metric Cameras for Measuring Works. *Journal of Physics: Conference Series*, Vol. 1118(1). https://doi.org/10.1088/1742-6596/1118/1/012044.

[30] Pengyu, H. O. U., Delu, C. H. E., Teng, L. I. U., Jiuping, Z. H. A. and Yunbin, Y. U. A. N., (2023). Status of Undifferenced and Uncombined GNSS Data Processing Activities in China. *Journal of Geodesy and Geoinformation Science*, Vol. 6(3), 135-144. https://doi.org/10.11947/j.JGGS.2023.0313.

[31] Elshewy, M., Hamdy, A. and Elsheshtawy, A., (2020). Improving the Accuracy of GNSS Data in the Absolute Point Positioning Based on Linear Relational Model. *International Journal of Geoinformatics*, Vol. 16(4), 51–57. https://journals.sfu.ca/ijg/index.php/journal/article/view/1797.

[32] Yun, S. and Lee, H., (2022). Experimental Analysis of GPS L2C Signal Quality under Various Observational Conditions. *International Journal of Geoinformatics*, Vol. 18(3), 21–37. https://doi.org/10.52939/ijg.v18i3.2199.

[33] Chen, X., Liu, H., Yu, B., Sheng, C., Huang, G., Hui, S. and Ying, J., (2024). BeiDou/GNSS Wide-Area Precise Positioning Technology and Service: Current Situation and Prospects. *Geomatics and Information Science of Wuhan University*. https://doi.org/10.13203/j.whugis20230472.

[34] Chymyrov, A., (2015). Precise Point Positioning (PPP) Services in Kyrgyzstan. *International Journal of Geoinformatics*, Vol. 11(4). https://journals.sfu.ca/ijg/index.php/journal/article/view/904.

[35] Noinak, M., Charoenphon, C., Weerawong, K., and Satirapod, C., (2022). Testing Horizontal Coordinate Correction Model Used for Transformation from PPP GNSS Technique to Thai GNSS CORS Network Based on ITRF2014. *International Journal of Geoinformatics*, Vol. 18(3), 55–64. https://journals.sfu.ca/ijg/index.php/journal/article/view/2203.

[36] Wu, Y. B., Liu, Y., Yi, W. and Ge, H. B., (2021). Impact of Elevation Mask on multi-GNSS Precise Point Positioning Performance. *Earth Science Informatics*, Vol. 14(3), 1111-1120. https://doi.org/10.1007/s12145-021-00619-0.

[37] Elsheikh, M., Iqbal, U., Noureldin, A. and Korenberg, M., (2023). The Implementation of Precise Point Positioning (PPP): A Comprehensive Review. *Sensors*, Vol. 23(21). https://doi.org/10.3390/s23218874.